Regulation of neuronal connexin-36 channels by pH

Daniel González-Nieto[a,b], Juan M. Gómez-Hernández[a], Belén Larrosa[a], Cristina Gutiérrez[a], María D. Muñoz[a], Ilaria Fasciani[a], John O'Brien[c], Agata Zappalà[d], Federico Cicirata[d], and Luis C. Barrio[a,1]

[a]Unit of Experimental Neurology, Department of Research, ''Ramón y Cajal'' Hospital, Carretera de Colmenar Viejo km 9, 28034-Madrid, Spain; [c]Department of Ophthalmology and Visual Science, University of Texas, 6431 Fannin, Houston, TX 77030; [d]Department of Physiological Science, University of Catania, Viale Andrea Doria 6, 95125-Catania, Italy; and [b]Bioengineering and Telemedicine Group, Politechnical University of Madrid, Ciudad Universitaria, 28040-Madrid, Spain

Edited by Michael V. L. Bennett, Albert Einstein College of Medicine, Bronx, NY, and approved September 12, 2008 (received for review April 30, 2008)

Neurotransmission through electrical synapses plays an important role in the spike synchrony among neurons and oscillation of neuronal networks. Indeed, electrical transmission has been implicated in the hypersynchronous electrical activity of epilepsy. We have investigated the influence of intracellular pH on the strength of electrical coupling mediated by connexin36 (Cx36), the principal gap junction protein in the electrical synapses of vertebrates. In striking contrast to other connexin isoforms, the activity of Cx36 channels decreases following alkalosis rather than acidosis when it is expressed in *Xenopus* oocytes and N2A cells. This uncoupling of Cx36 channels upon alkalinization occurred in the vertebrate orthologues analyzed (human, mouse, chicken, perch, and skate). While intracellular acidification caused a mild or moderate increase in the junctional conductance of virtually all these channels, the coupling of the skate Cx35 channel was partially blocked by acidosis. The mutational analysis suggests that the Cx36 channels may contain two gating mechanisms operating with opposing sensitivity to pH. One gate, the dominant mechanism, closes for alkalosis and it probably involves an interaction between the C- and N-terminal domains, while a secondary acid sensing gate only causes minor, albeit saturating, changes in coupling following acidosis and alkalosis. Thus, we conclude that neuronal Cx36 channels undergo unique regulation by pH_i since their activity is inhibited by alkalosis rather than acidosis. These data provide a novel basis to define the relevance and consequences of the pH-dependent modulation of Cx36 synapses under physiological and pathological conditions.

alkalosis | electrical synapses | intracellular pH | pH gating | gap junction

Gap junction channels are the structural basis of the synapses that provide a low resistance pathway for direct electrical signaling between neurons (1). The discovery of mammalian connexin36 genes (Cx36) and their vertebrate orthologues, the first connexin isoform with a preferential expression in neurons (2–6), has considerably advanced our understanding of the prevalence and physiological importance of electrical neurotransmission. Cx36 is expressed strongly during development and although it is more weakly expressed in adults, it persists in specific neurons in the retina, hippocampus, neocortex, inferior olive, several brain-stem nuclei, and spinal cord, among others. Cx36 has been identified at ultrastructurally defined electrical synapses in many neuronal types that are believed to be electrically coupled (7–11). However, despite the prevalence of Cx36, some central neurons may be coupled by other connexins (12). Electrical synapses have been implicated in several physiological aspects of brain function and in anomalous population activities characteristic of epilepsy (13, 14). Mice lacking the Cx36 gene showed very little electrical coupling between hippocampal and neocortical interneurons and disruption of the 30–80 Hz γ-oscillations (15, 16). In addition, fewer sharp wave high-frequency (approximately 200 Hz) ripple oscillations and attenuation of epileptiform discharges evoked by 4-aminopyridine have also been reported in hippocampal slices (17). Cx36 knock-out mice provide evidence that Cx36 synapses synchronize spikes in several areas, including the thalamic reticular nucleus (18), inferior olive (19), mitral cells of the olfactory bulb glomeruli (9), suprachiasmatic nucleus (20), and locus coeruleus (10). In the retina, the loss of Cx36 causes deficient scotopic vision due to the impairment of electrical synapses in the rod pathway (21).

A fundamental aspect of electrical neurotransmission mediated by Cx36 is its plasticity, given that the conductance of the constitutive neuron-to-neuron channels formed can be easily regulated (22–25). However, the sensitivity of Cx36 synapses to the intracellular proton ion concentration has not yet been studied in detail. The intracellular pH of central mammalian neurons can acidify or alkalinize by tenths of a pH unit under physiological conditions and in numerous pathological situations (26). We have quantified the effects of intracellular pH (pH_i) on Cx36 junctions using *in vitro* systems, and we found that unlike other connexins, alkalinization rather than acidification reduces the junctional conductance of Cx36 channels from all vertebrate species tested. Structural components involved in this novel kind of pH gating have been identified.

Results

Intracellular Alkalinization Inhibits the Activity of Cx36 Channels. Intracellular acidification and alkalinization exert opposite effects on the conductance (G_j) of Cx43 and Cx36 junctions (Fig. 1). Acidification with 100% CO_2 produces a drop in the pH_i from 7.24 to 6.49 and causes complete and reversible uncoupling of rat Cx43 oocyte pairs (27). By contrast, this change in pH_i somewhat increased the G_j of human (h) Cx36 to 112.47 ± 1.35% ($n = 12$; Student's t test $P < 0.05$) of its value at the resting pH_i. Conversely, while alkalinization of the pH_i to 7.91 slightly increases the G_j of Cx43 (112.90 ± 2.3%; $n = 9$, $P < 0.05$), it reduced the G_j of hCx36 to 39.4 ± 1.7% of the resting value. Again, alkalinization induced uncoupling was reversed when the pH_i returned to the control level after washing with a pH 7.40 solution. Similarly, hCx36 channels expressed in *N2A* cells responded to alkalosis (pH_i approximately 7.83) with a reversible blockage of coupling by 52.6 ± 1.8%, while acidosis (pH_i approximately 6.37) caused a small increase in G_j (109.05 ± 3.4%; $n = 10$, $P < 0.05$). The pH-dependent changes in G_j were similar in magnitude to those observed in oocytes but they followed a faster time course of 1–3 min, reflecting the more rapid variations of pH_i in N2A cells. The pH_i sensitivity of hCx36 channels can be described by a monotonic curve with a half channel activation at a pK_H 7.86 (Fig. 2). Indeed, above the reference value at a resting pH_i approximately 7.24, G_j increased

Author contributions: D.G.-N. and L.C.B. designed research; D.G.-N., J.M.G.-H., B.L., C.G., M.D.M., and I.F. performed research; J.O., A.Z., and F.C. contributed cloning and cDNA constructs; D.G.-N., J.M.G.-H., and B.L. analyzed data; and L.C.B. wrote the paper.

The authors declare no conflict of interest.

This article is a PNAS Direct Submission.

[1]To whom correspondence should be addressed at: Unidad de Neurología Experimental, Departamento de Investigación, Hospital ''Ramón y Cajal'', Carretera de Colmenar km 9, 28034-Madrid, SPAIN. E-mail: luis.c.barrio@hrc.es.

This article contains supporting information online at www.pnas.org/cgi/content/full/0804189105/DCSupplemental.

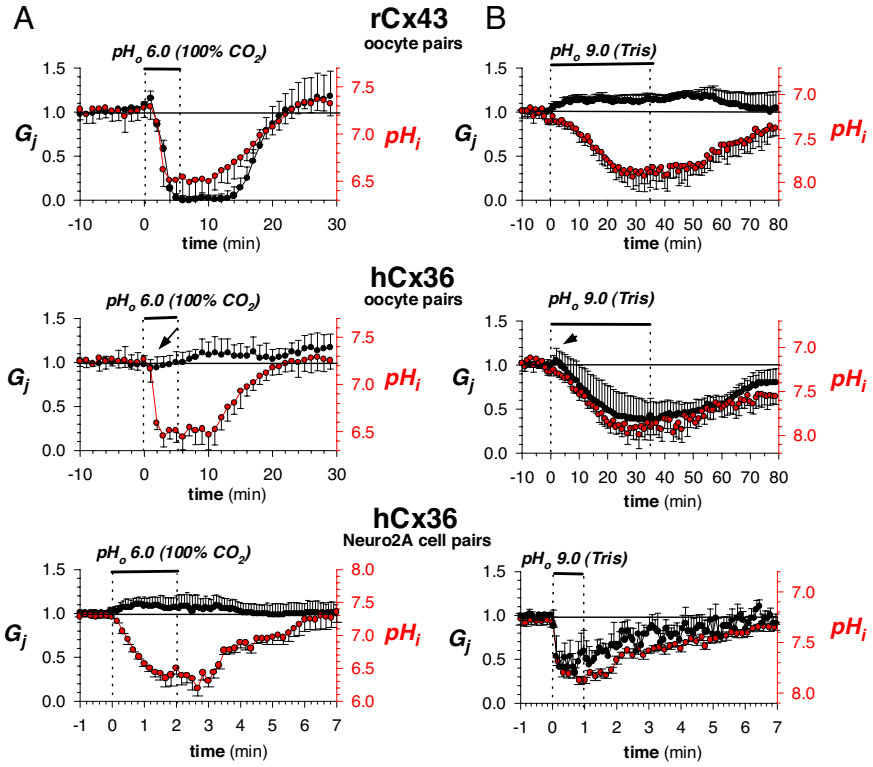

Fig. 1. Alkalinization reduces the electrical coupling mediated by neuronal Cx36 channels. Cell pairs coupled through rat connexin43 (rCx43) and human connexin36 (hCx36) junctions that were exposed first to control medium (pH$_o$ 7.40) and then superfused with acidic or basic solutions (bars) before again switching them to the control medium while the junctional conductance (G_j; black) was monitored and the pH$_i$ (pH_i; red) was measured with SNARF-1. G_j was normalized relative to its value at the resting pH$_o$. (*A*) Acidification typically causes a rapid and reversible uncoupling of Cx43 (*Upper*) but it slightly increases the Cx36 G_j between the oocyte (*Middle*; $n = 12$, $P < 0.05$) and *N2A* cell pairs (*Bottom*; $n = 10$, $P < 0.05$). (*B*) Alkalinization produces a mild increase in Cx43 coupling (*upper*; $n = 9$, $P < 0.05$) yet it reversibly reduces the G_j for Cx36. Note that the G_j in the Cx36 oocytes tends to decrease somewhat before it increases upon acidosis (arrow), while a small increase in G_j typically precedes the uncoupling with alkalosis (arrowhead). Data in Figs. 1–5 represent the mean values ± SE. ($n = 9$–12).

to a maximum of the 128.28 ± 12.46% at pH$_i$ 5.66 while it decreased in a more pronounced manner in the basic direction to 27.83 ± 8.5% at pH$_i$ 8.16.

The human Cx36 gene has easy recognizable orthologues across the vertebrate phyla (2–6). Alkalinization-induced uncoupling was observed in all of the channels analyzed including:

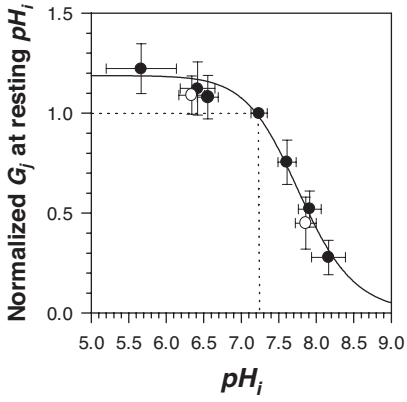

Fig. 2. pH$_i$ sensitivity of human Cx36 junctions. The curve was constructed with the steady state values of G_j in oocytes (●) and in N2A cells (○) after stabilization of the pH$_i$ value following each pH stimulus ($n = 12$). The average G_j/pH_i relationship was fitted with a four-parameter sigmoidal function of the form: $G_j = G_{jmax}/(1+\exp(\text{slope}(pHi-pK_H))$, where G_j is maximal at the acidic extreme ($G_{jmax} = 1.17$) and decreases in the alkalotic direction with a midpoint channel activity parameter pK_H of 7.86.

mouse Cx36 (m), chicken 35.1 (ch), skate (s), and perch (p) Cx35 (Fig. 3). Like hCx36, the blockage at pH$_i$ 7.92 was pronounced in mCx36 and pCx35 junctions, which decreased the G_j to 39.5 ± 2.5% and 27.0.5 ± 1.9%, respectively, while the G_j of chCx35.1 (50.5 ± 0.8%) and sCx35 (56.4 ± 1.4%) was less sensitive. Acidification with 100% CO$_2$ (pH$_i$ 6.48) caused a minor increase in the G_j of mCx36 and pCx35 (to 109.9 ± 0.4% and 107.7 ± 0.3%; $n = 9$, $P < 0.05$), as in hCx36, and a somewhat greater increase in chCx35.1 (to 138.9 ± 2.3%; $n = 9$, $P < 0.05$). By contrast, acidosis induced a rapid partial uncoupling of sCx35 that was saturated at 88.2 ± 2.3% ($n = 9$, $P < 0.05$).

Molecular Mechanisms of pH Gating. To identify the structural components involved in the regulation by pH, various mutations were generated within the three cytoplasmic domains of hCx36. Of these, the H18Q substitution at the amino-terminal domain (NT-H18Q) and the deletion of residues L282-V321 at the distal portion of the carboxy-terminal domain (CT-L282stop) altered pH sensitivity in the same way (Figs. 4 and 5). Both mutant channels responded to extreme alkalinization (pH$_i$ 8.20) with a modest increase in G_j (to 116.3 ± 2.8% for H18Q and 113.6 ± 5.1% for L282stop; $n = 12$, $P < 0.05$), in striking contrast with the uncoupling effect observed in the wild-type junctions (to 26.5 ± 2.5%, Fig. 4*A*). For extreme acidosis (pH$_i$ 5.73), the minor increase in the wild-type G_j (to 125.7 ± 11.3%; $n = 12$, $P < 0.05$) also disappeared in these mutants and was substituted by a small yet rapid reduction in G_j (to 76.5 ± 2.1% in the NT-H18Q mutant and 85.1 ± 3.2% for the CT-L282stop mutant; $n = 12$, $P < 0.05$, Fig. 4*B*). In summary, these two mutations abolished the gating responsible for the reduction in G_j upon alkalosis and

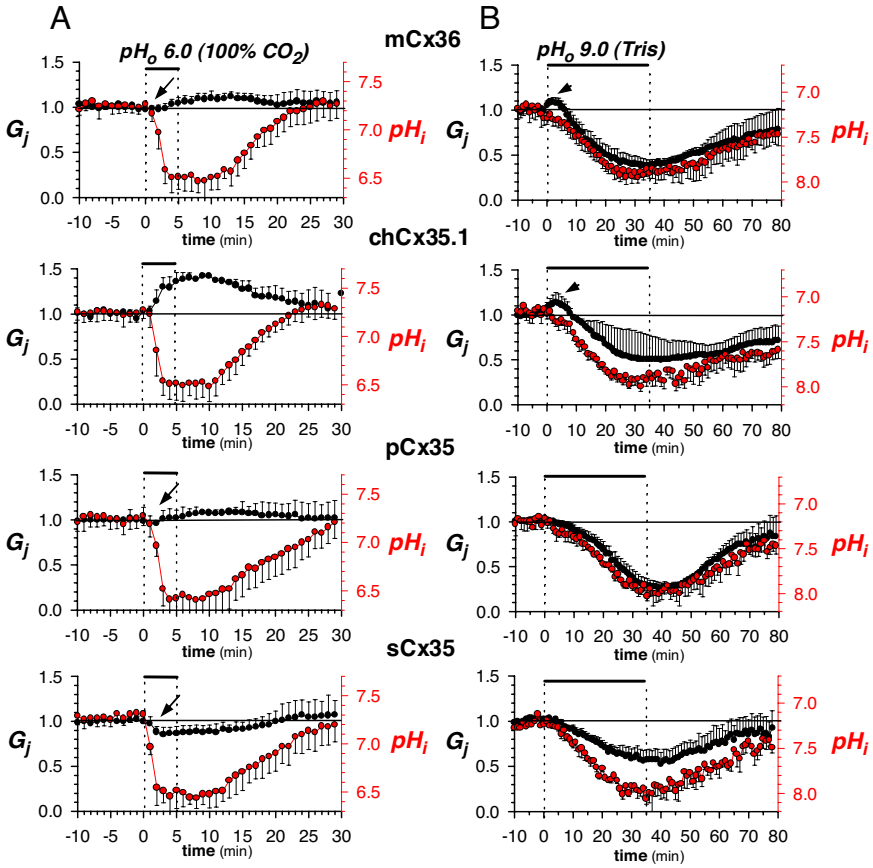

Fig. 3. Alkalinization-induced uncoupling is common among Cx36 orthologues. Oocytes were injected with the RNAs encoding for mouse Cx36 (mCx36), chicken Cx35.1 (chCx35.1), perch Cx35 (pCx35), and skate Cx35 (sCx35). (*A*) Intracellular acidification induced small increases in the G_j of mCx36 and pCx35 and a moderate rise in chCx35.1, while the G_j of sCx35 decreased slightly ($n = 9$, $P < 0{,}05$). (*B*) By contrast, alkalization caused a marked reduction in the G_j of mCx36 and pCx35 and a moderate decrease in chCx35.1 and sCx35. Arrows and arrowheads as in Fig. 1.

the increase following acidosis. Moreover, these mutations unmasked a novel acidic sensitivity that only caused minor changes in G_j but in the opposite direction (Fig. 5*A*). The deletion of residues S101-Q155 in the cytoplasmic loop (CL-delS101-Q155) significantly reduced the junctional conductance at the resting pH (wt: 2.54 ± 0.57 μS vs. delS101-Q155: 0.39 ± 0.21 μS; $n =$ 23 pairs, $P < 0.01$), although it induced a larger increment in G_j in response to acidosis than the wild type at this pH$_i$ (approximately 7.5 fold at pH$_i$ 5.84, Figs. 4*B* and 5*B*). For alkalosis (pH$_i$ 8.18), G_j decreased to 21.6 ± 1.2%, which was only slightly smaller that the wild-type coupling. Thus, this mutation shifted the pH sensitivity curve toward the acid side by more than one pH unit (from a pK_H 7.86 to 6.67), while the slope of curve did not change significantly (Fig. 5*B Inset*). Such a displacement justifies the low levels of coupling observed at the resting pH. The double delS101-Q155 and H18Q mutant was indistinguishable from the single H18Q mutant described above (data not shown). Hence, the shift in the pH curve caused by the delS101-Q155 mutation can be exclusively attributed to an effect on the alkalotic mechanism. The deletion of residues R182-V204 at the carboxyl extreme of CL domain did not yield functional channels, while the deletion of residues N156-S185 in the middle of CL domain did not affect channel formation or modify regulation by pH (data not shown).

Discussion

We show here that the neuronal channels made up of human and mouse Cx36, chicken Cx35.1, and perch and skate Cx35 are inhibited by alkalosis, in striking contrast to channels comprised of other connexin isoforms whose conductance decreases upon acidosis (28). Alkalinization-induced uncoupling is similar in hCx36, mCx36, and pCx35 and somewhat less marked in chCx35.1 and sCx35. Conversely, acidosis at pH$_i$ approximately 6.5 results in a mild increase in the conductance of hCx36, mCx36, and pCx35 channels (to approximately 110–115%) and a moderate increase in chCx35.1 channels (to approximately 140%). The sole exception is that of sCx35 junctions, which clearly show a biphasic pH dependence since their conductance also decreases following acidosis, albeit in a less pronounced manner than after alkalosis. Recently, this kind of dual pH sensitivity has also been observed in the gap junctions of cardiac myocytes (29). In previous studies *in vitro*, wherein the effect of alkalization was not explored and the experiments were carried out without measuring the pH$_i$, a partial uncoupling effect of acidosis on sCx35 was also observed (22). By contrast, full uncoupling of mCx36 was reported following the application of 100% CO_2, although this was probably due to channel rundown since there was no recovery of coupling after washout (figure 6 in ref. 30).

The remarkable conservation of the regulation of Cx36 orthologues by pH$_i$ suggests the presence of fundamental mechanistic and structural components. Mutagenesis of hCx36 suggests the existence of two distinct mechanisms controlling the response to changes in pH: principally, an alkali gate and secondarily, an acidic gate. The absence of hysteresis in the G_j/pH_i relationships for alkalinization and the subsequent reacidification, and for the inverse process (Fig. 5), indicate a direct effect of pH$_i$ on the channel protein. Alkalotic gating was abolished by

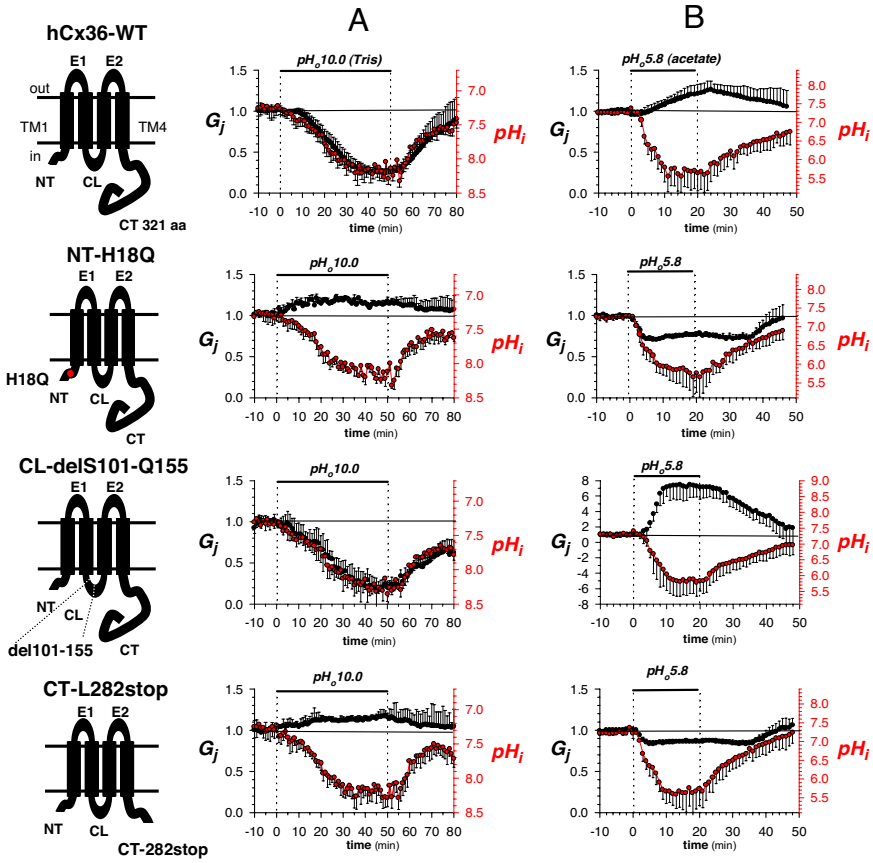

Fig. 4. Mechanisms of pH gating. Human Cx36 was mutated in its three cytoplasmic domains (*Left Column*) by creating the H18Q substitution in the NT-domain (NT-H18Q), the deletion of residues S101 to Q155 in the cytoplasmic loop (CL-delS101-Q155), and a truncation of the CT-domain at position 282 (CT-L282stop). The NT-H18Q and CT-L282stop mutations abolished the uncoupling at alkalosis (*A*) and the mild increase in G_j following acidosis of wild type junctions (HCx36wt) (*B*). Moreover, these mutations induced a novel pH regulation characterized by minor increases and decreases with alkalosis and acidosis, respectively ($n = 12$, $P < 0.05$). The CL-delS101-Q155 mutation reduced the G_j for alkalosis to a similar level as in the wild type and induced a large increment in the G_j following acidosis.

either of the two mutations, the NT-H18Q and the CT-L282stop. Mechanistically, a simple interpretation of these data is that the NT- and CT-domains may interact under alkalotic conditions to close the channel. Functional and structural studies conducted mainly in Cx43 have led to the proposal that acidic pH gating follows a "particle-receptor" model, in which the CT-domain acts as a "gating particle" that binds in a pH-dependent manner to a specific region in the CL-domain (acting as a "receptor"), thereby occluding the channel pore (27, 31, 32). The location of the alkaline pH sensor remains elusive in our study, although the marked shift of the titration curve toward the acidic side caused by the CL-delS101-Q155 mutation suggests that this particular region of the CL would exert a strong influence over the proton sensor of wild type channels. In the two-gate model of Cx36 channels, the acidic pH gating unmasked by the NT-H18Q and CT-L282stop mutations could partially counteract the effects mediated by the alkalotic mechanism, and this may be responsible for the small biphasic changes in G_j observed in the wild type hCx36 channels. The acidic gate can also explain the net effect of uncoupling upon acidosis of sCx35, since in these particular channels the contribution of the alkalotic mechanism at an acidic pH is negligible [supporting information (SI) Fig. S1].

The cytoplasmic domains of Cx36 involved in the alkalotic mechanism of pH have also been implicated in channel trafficking and other forms of gating. Indeed, the four most C-terminal amino acids are directly implicated in the binding of the zonula occludens-1 scaffolding protein (33) and more proximally, a calmodulin binding site was mapped to residues 273–291 (34). Furthermore, the protein kinase A-mediated phosphorylation of Cx36 that induces uncoupling occurs at S293 and S110 of the CT- and CL-domains (25). These multiple functions raise the possibility of dynamic interactions between pH gating and other regulatory mechanisms, as reported for other connexins (35, 36). In this respect, we found that the voltage gating properties of wild type Cx36 junctions did not vary significantly at low or high pH values, and the mutations in Cx36 that eliminate or alter the alkalotic mechanism of pH apparently leave the voltage sensitivity intact (Figs. S2 and S3).

The intracellular proton concentration exerts profound effects on neuronal excitability and brain function, but the exact contribution of the pH-dependent modulation of electrical neurotransmission is still to be determined. Accordingly, the alkalotic pH sensitivity *in vitro* reported here indicates that the modulation of Cx36 synapses by pH_i cannot be anticipated by the general rule derived from other connexins, whose channels tend to close following acidification. Conversely, the G_j/pHi curve for hCx36 channels with a half-maximal activation around a pH_i 7.86 predicts a modest enhancement of electrical transmission under extreme acidic conditions and more pronounced reductions with pH_i deviations in the alkalotic direction. Given the widespread distribution of Cx36-mediated synapses in the mammalian cen-

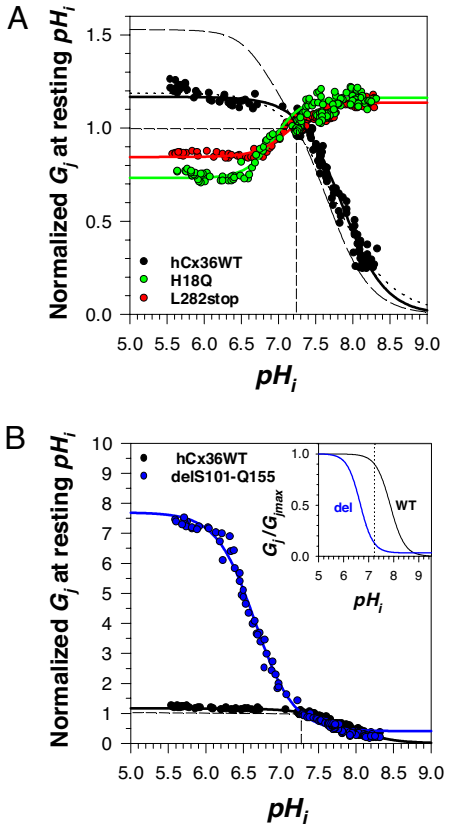

Fig. 5. Comparison of the pH_i sensitivity of mutant and wild-type hCx36 channels. The pH_i/G_j relationships of the data shown in Fig. 4 were constructed by plotting the changes in G_j along the time course of alkalinization and subsequent re-acidification, and vice versa. (*A*) The dynamic pH_i/G_j relationships of wild type junctions (solid black line) did not differ significantly from the steady state curve shown in Fig. 2 (dotted line). The pH_i sensitivity of NT-H18Q (green) and CT-L282stop (red) channels is similar, with minor albeit saturating changes in G_j in the opposite pH direction to those of the wild type. The curves can be described with a regular Hill equation (solid lines) of the form $G_j = G_{jmax}/(1+pK_a/pH_i)^h + G_{jmin}$ and with the parameters for NT-H18Q of maximal G_{jmax} and minimal G_{jmin} conductance of 1.16 and 0.7, a midpoint channel activity $pK_a = 7.15$, and with a Hill coefficient $h = 3.7$ and the parameters of $G_{jmax} = 1.14$ and $G_{jmin} = 0.8$, a $pK_a = 6.94$ and a $h = 3.3$ for the CT-L282stop mutant. The theoretical titration curve for the alkalotic mechanism suppressed by these two mutants corresponds to a Hill equation with a $G_{jmax} = 1.36$, a G_{jmin} near zero, a $pK_a = 7.57$ and a $h = 2.6$ (broken black line). (*B*) The curve for CL-delS101-Q155 channels (blue) shows a large increase of G_j for acidosis in concordance with the displacement of pK_H 7.86 to 6.68 (*Inset*).

tral nervous system, this kind of pH-dependence could regulate the strength of electrical transmission in every major region of the brain and retina. Outside of nervous tissue, Cx36 also mediates electrical coupling in the β-cells of pancreatic islets wherein it plays an important regulatory role in the control of insulin secretion (37). Since the electrical synapses formed by Cx36 channels do not close upon acidosis, neurons expressing Cx36 may remain coupled even if the pH_i drops (38), as happens during retinal or brain ischaemia, and the spreading depression. On the other hand, the hyperventilation (hypocapnia) used clinically to detect epilepsy, and certain compounds such as ammonium ions, would be expected to reduce Cx36-mediated neurotransmission by virtue of raising the pH in the interior of cells. Although no mutations in the amino acid sequence have yet been found, there is evidence of an allelic and genotypic association of the Cx36 gene with juvenile myoclonic epilepsy (39).

Methods

DNA Constructs. While total RNA from adult mouse brain and chicken embryos (developmental stage HH17) was extracted according to the manufacturer's instructions (Invitrogen-Life Technologies), total RNA from human brain was obtained commercially (Ambion). Reverse transcription and amplification of cDNA by PCR (PCR) was carried out using the Access RT-PCR system (Promega) with slight modifications and the primer sequences are shown in Table S1. For oocyte expression, cDNA fragments encoding human Cx36 (966 bp, GenBank Accession number: AF153047; ref. 6), mouse Cx36 (966 bp, AF016190; ref. 5), chicken Cx35.1 (915 bp, AY700221) and skate Cx35 (909 bp; U43290; ref. 2) were inserted into the pBSXG vector (40). The original perch Cx35 cDNA construct (915 bp; AF059183) cloned into a pcDNA 3.1 Zeo (+) vector was also used in this study (4). Human Cx36 cDNA was subcloned into the bicistronic pIRES2-EGFP vector (Clontech) for transfection into the N2A cell line. Site-directed mutagenesis of hCx36 and sCx35 cDNA in the pBSXG vector was performed by PCR with modified primers that annealed back-to-back and that amplified the whole vector (as indicated in Table S2).

Expression Systems. Isolation of *Xenopus laevis* oocytes and cRNA synthesis and its injection were performed as described previously (41). Oocytes were injected with the cRNA encoding Cx36 and rCx43 (0.5–1.0 μg/μl, 50 nl/oocyte) mixed with an antisense Cx38 oligonucleotide (15 ng/oocyte) to block endogenous expression of this connexin. The murine neuroblastoma 2A cell line (*N2A*; ATCC, CCL131) was cultured and transfected with the pIRES-hCx36-EGFP vector as described previously (42).

Electrophysiology and pH_i Measurement. Junctional conductance (g_j) was measured by the double dual-electrode voltage-clamp technique in oocytes (41) and by the dual whole-cell patch clamp technique in the EGFP-positive *N2A* cell pairs (23). The microelectrodes for oocytes were filled 3 M KCl, 1 mM EGTA, 5 mM Hepes, pH 7.15 and had a resistance of approximately 0.5 MΩ. The patch electrodes had a resistance of approximately 5 MΩ when filled with (in mM) 120 K-aspartate, 10 NaCl, 1 $CaCl_2$, 1 $MgCl_2$, 10 EGTA, 5 ATP, 5 Hepes, pH 7.20. Cell pairs were placed into a recording chamber (1 ml) and first superfused with control media (pH 7.40) at a flow rate of 3 ml/min and then with the acidic or basic solutions. Once the new stable pH_i was reached, they were again switched to control pH medium. The g_j was monitored by applying repetitive transjunctional voltage pulses of +20 mV, 500 ms and 0.016 Hz at a holding potential of −40 mV in oocytes, and of −20 mV, 200 ms and 0.1 Hz at 0 mV in *N2A* cells. Paired oocytes with g_j values of 0.5–5 μS and *N2A* cell pairs with values of 0.77 ± 0.25 nS were included in the study. The external control solution (pH_o 7.40) was ND96 medium for the oocytes (in mM: 96 NaCl, 2 KCl, 1 $MgCl_2$, 1.8 $CaCl_2$, and 5 Hepes- or 20 Tris-buffer), while the bath solution for the *N2A* cells was (in mM): 140 NaCl, 4 KCl, 2 CsCl, 2 $CaCl_2$, 1 $MgCl_2$, 1 $BaCl_2$, 2 pyruvate, 5 glucose, and 5 Hepes- or 10 Tris-buffer. Intracellular acidification was achieved by superfusion with Hepes-buffered solutions saturated with 100% CO_2 (pH_o 6.0), a bicarbonate-buffered solution containing 5 mM $NaHCO_3$ and 5% CO_2 (pH_o 6.5), and with a sodium acetate-solution (in mM: 103 sodium acetate, 20 NaCl, 1 KCl, 2.4 $NaHCO_3$, 0.82 $MgSO_4$, 0.74 $CaCl_2$ and 20 Hepes, pH_o 5.8). The Tris-buffered saline solutions were prepared by adding the appropriate amounts of Trizma HCl and Trizma base (Sigma) to adjust the pH_o to 7.4, 8.0, 9.0 and 10.0. All experiments were performed at 22–24 °C.

Carboxy-seminaphthorhodafluor-1 (C-SNARF-1; Invitrogen) was used to measure pH_i. Oocytes were injected with the dextran-SNARF-1 (MW 70,000; 357 μM) mixed with the cRNA 2–3 days before recording, while the *N2A* cells were loaded with the cell-permeant SNARF-1 acetoxymethyl ester (5 μM) and recorded within the following 2 h. Two regions of interest (ROI) were defined, one inside the cell for pH_i and another outside for the background signal. In the oocytes, the ROIs were 15 × 150 μm in size (2250 pixels) and the intracellular ROI was placed near to the cell-to-cell contact area, while the ROIs in *N2A* cells were the size of the cell (approximately 12 μm of diameter; 240 pixels). Using the 568-nm excitation line of a krypton-argon laser confocal microscope (MRC-1024, BioRad), the fluorescence emitted from the ROIs at wavelengths of 570/40 nm and 640/40 nm was collected by two independent photodetectors (255-gray levels), every 1 min in oocytes and every 10 s in N2A cells. After background subtraction, the mean fluorescence intensities at the two emissions were used to obtain the 640/570 ratios that were converted to pH values against the intracellular calibration pH (43). The accuracy of the pH dependence of the emission ratios was preserved in the pH_i range of 5.5 to 8.5.

ACKNOWLEDGMENTS. We thank Rosa Barquero for her excellent technical assistance. This work was supported by grants from the Spanish Ministry of Science and Technology (SAF2001–0048; SAF2005–03414 and CSD2008_00005), and the Community of Madrid (MADR_IB, S2006/SAL-0312) to L.C.B.

1. Bennett MVL (1977) in *Handbook of Physiology. The Nervous System*, ed. Kandel ER (Williams and Wilkins, Baltimore), pp. 357–416.
2. O'Brien J, Al-Ubaidi MR, Ripps H (1996) Connexin 35: A gap-junctional protein expressed preferentially in the skate retina. *Mol Biol Cel* 7:233–243.
3. Condorelli DF, *et al.* (1998) Cloning of a new gap junction gene (Cx36) highly expressed in mammalian brain neurons. *Eur J Neurosci* 10:1202–1208.
4. O'Brien J, Bruzzone R, White TW, Al-Ubaidi MR, Ripps H (1998) Cloning and expression of two related connexins from the perch retina define a distinct subgroup of the connexin familiy. *J Neurosci* 18:7625–7637.
5. Söhl G, Degen J, Teubner B, Willecke K (1998) The murine gap junction gene connexin 36 is highly expressed in mouse retina and regulated during brain development. *FEBS Lett* 428:27–31.
6. Belluardo N, Trovato-Salinaro A, Mudo G, Hurd YL, Condorelli DF (1999) Structure, chromosomal localization, and brain expression of human Cx36 gene. *J Neurosci Res* 57:740–752.
7. Rash JE, *et al.* (2000) Immunogold evidence that neuronal gap junctions in adult rat brain and spinal cord contain connexin-36 but not connexin-32 or connexin-43. *Proc Natl Acad Sci USA* 97:7573–7578.
8. Fukuda T, Kosaba T, Singer W, Galuske RA (2006) Gap junctions among dendrites of cortical GABAergic neurons establish a dense widespread intercolumnar network. *J Neurosci* 26:3434–3443.
9. Christie JM, *et al.* (2005) Connexin36 mediates spike synchrony in olfactory bulb glomeruli. *Neuron* 46:761–772.
10. Rash JE, *et al.* (2007) Identification of connexin36 in gap junctions between neurons in rodent locus coeruleus. *Neuroscience* 147:938–956.
11. Hamzei-Sichani, *et al.* (2007) Gap junctions on hippocampal mossy fiber axons demonstrated by thin-section electron microscopy and freeze-fracture replica immunogold labeling. *Proc Natl Acad Sci USA* 104:12548–12553.
12. Söhl G, Maxeiner S, Willecke K (2005) Expression and functions of neuronal gap junctions. *Nat Rev Neurosci* 6:191–200.
13. Bennett MVL, Zukin S (2004) Electrical coupling and neuronal synchronization in the mammalian brain. *Neuron* 41:495–511.
14. Traub RD, Contreras D, Whittington MA (2005) Combined experimental/simulation studies of cellular and network mechanisms of epileptogenesis *in vitro* and *in vivo*. *J Clin Neurophysiol* 22:330–342.
15. Deans M, Gibson JR, Sellitto C, Connors BW, Paul DL (2001) Synchronous activity of inhibitory networks in neocortex requires electrical synapses containing connexin 36. *Neuron* 31:477–485.
16. Hormuzdi SG, *et al.* (2001) Impaired electrical signaling disrupts gamma frequency oscillations in connexin 36-deficient mice. *Neuron* 31:487–495.
17. Meier C, *et al.* (2002) Reduction of high-frequency network oscillations (ripples) and pathological networks discharges in hippocampal slices from connexin 36-deficient mice. *J Physiol (London)* 541:521–528.
18. Landisman CE, *et al.* (2002) Electrical synapses in the thalamic reticular nucleus. *J Neurosci* 22:1002–1009.
19. Long MA, Deans MR, Paul DL, Connors BW (2002) Rhythmicity without synchrony in the electrically uncoupled inferior olive. *J Neurosci* 22:10898–10905.
20. Long MA, Jutras MJ, Conners BW, Burwell RD (2005) Electrical synapses coordinate activity in the suprachiasmatic nucleous. *Nat Neurosci* 8:61–66.
21. Güldenagel M, *et al.* (2001) Visual transmission deficits in mice with targeted disruption of the gap junction gene connexin36. *J Neurosci* 21:6036–6044.
22. White TW, *et al.* (1999) Functional characteristics of skate connexin35, a member of the γ subfamily of connexins expressed in the vertebrate retina. *Eur J Neurosci* 11:1883–1890.
23. Srinivas M, *et al.* (1999) Functional properties of channels formed by the neuronal gap junction protein connexin36. *J Neurosci* 19:9848–9855.
24. Pereda A, *et al.* (1998) Ca^{2+}/calmodulin-dependent kinase II mediates simultaneous enhancement of gap junctional conductance and glutamatergic transmission. *Proc Natl Acad Sci USA* 95:13272–13277.
25. Urschel S, *et al.* (2006) Protein kinase A-mediated phosphorylation of connexin36 in mouse retina results in decreased gap junctional communication between AII amacrine cells. *J Biol Chem* 281:33163–33171.
26. Chesler M (2003) Regulation and modulation of pH in the brain. *Physiol Rev* 83:1183–1221.
27. Morley GE, Taffett SM, Delmar M (1996) Intramolecular interactions mediate pH regulation of connexin-43 channels. *Biophys J* 70:1294–1302.
28. Harris LH (2001) Emerging issues of connexin channels: Biophysics fills the gap. *Q Rev Biophys* 34:325–472.
29. Swietach P, Rosini A, Spitzer KW, Vaughan-Jones RD (2007) H^+ ion activation and inactivation of the ventricular gap junction. *Circ Res* 100:1045–1054.
30. Teubner B, *et al.* (2000) Functional expression of the murine connexin 36 gene coding for a neuron-specific gap junctional protein. *J Membr Biol* 176:249–262.
31. Duffy HS, *et al.* (2002) pH-dependent intramolecular binding and structure involving Cx43 cytoplasmic domains. *J Biol Chem* 277:36706–36714.
32. Hirst-Jensen B, Sahoo P, Kieken F, Delmar M, Sorgen PL (2007) Characterization of the pH-dependent interaction between the gap junction protein connexin43 carboxyl terminus and cytoplasmic loop domains. *J Biol Chem* 282:5801–5813.
33. Li X, *et al.* (2004) Neuronal connexin36 association with zonula occludens-1 protein (ZO-1) in mouse brain and interaction with the first PDZ domain of ZO-1. *Eur J Neurosci* 19:2132–2146.
34. Burr GS, Mitchell CK, Keflemariam YJ, Heidelberger R, O'Brien J (2005) Calcium-dependent binding of calmodulin to neuronal gap junction proteins. *Biochem Biophys Res Commun* 335:1191–1198.
35. Peracchia C (2004) Chemical gating of gap junction channels. Roles of calcium, pH and calmodulin. *Biochim Biophys Acta* 1662:61–80.
36. Duffy HS, *et al.* (2004) Regulation of connexin43 protein complexes by intracellular acidification. *Circ Res* 94:215–222.
37. Wellershaus K, *et al.* (2008) A new conditional mouse mutant reveals specific expression and functions of connexin36 in neurons and pancreatic beta-cells. *Exp Cell Res* 314:997–1012.
38. Hampson ECGM, Vaney DI, Weiler R (1992) Dopaminergic modulation of gap junction permeability between amacrine cells in mammalian retina. *J Neurosci* 12:4911–4922.
39. Mas C, *et al.* (2004) Association of the connexin36 gene with juvenile myoclonic epilepsy. *J Med Genet* 41:e93.
40. Martin P, *et al.* (1998) Assembly of chimeric-aequorin into functional proteins into functional gap junction channels. *J Biol Chem* 273:1719–1726.
41. Barrio LC, *et al.* (1991) Gap junctions formed by connexin 26 and 32 alone and in combination are differently affected by applied voltage. *Proc Natl Acad Sci USA* 8:8410–8414.
42. González D, Gómez-Hernández JM, Barrio LC (2006) Species specificity of mammalian connexin26 to form open voltage-gated hemichannels. *FASEB J* 20:2329–2338.
43. Blank PS, *et al.* (1992) Cytosolic pH measurements in single cardiac myocytes using carboxy-seminaphthorhodafluor-1. *Am J Physiol* 263:H276–H284.